Analysis of Nonreciprocal Coupled Image Lines

DAVID B. SILLARS, MEMBER, IEEE, AND LIONEL E. DAVIS, SENIOR MEMBER, IEEE

Abstract—**The effective dielectric constant method is used to analyze the nonreciprocal coupling properties of coupled image lines separated by a longitudinally magnetized ferrite slab. Two structures are considered, one incorporating low-dielectric-constant image lines ($\epsilon_r = 2.56$), the other incorporating image lines consisting of high-dielectric-constant material ($\epsilon_r = 9.8$). Results of dispersion characteristics, coupling parameters, and field distributions are presented.**

I. Introduction

A NUMBER OF millimeter-wave nonreciprocal components have recently been developed utilizing dielectric waveguide technology. Devices such as resonance isolators, junction circulators [1], and Reggia–Spencer-type phase shifters [1], [2] have been fabricated. The modes of operation of these devices are based on principles similar to traditional waveguide designs [3]. More novel devices have exploited the nonreciprocal coupling phenomenon present in distributed coupled line structures, such as that between a dielectric image line and a ferrite slab, to develop an isolator [4], [5]. Similarly, a 4-port circulator can be produced from the nonreciprocal coupling behavior between two image lines with a transversely magnetized ferrite overlay placed on top [6].

These devices have been developed to help alleviate the problems of requiring small ferrites when operating at millimeter-wave frequencies. They do however, require large external magnets from which to obtain the applied magnetic field strengths necessary to saturate the ferrites. One solution to this problem is to use hexagonal ferrite materials which have high internal magnetic field strengths, such as those used in the devices described in [1]. At present such materials are not widely available. However, an alternative solution is to incorporate longitudinally magnetized ferrite slabs into distributed coupled line structures. Due to the small demagnetizing factor which results when ferrite slabs are magnetized along their length, only small applied field strengths are required to saturate the ferrites. Isolators and a 4-port circulator have been developed in coupled-slot finlines incorporating longitudinally magnetized ferrites [7]. Also recently, initial experimental results have shown nonreciprocal coupling behavior occurring between two image lines separated by a longitudinally magnetized ferrite slab of the type shown in Fig. 1 [8].

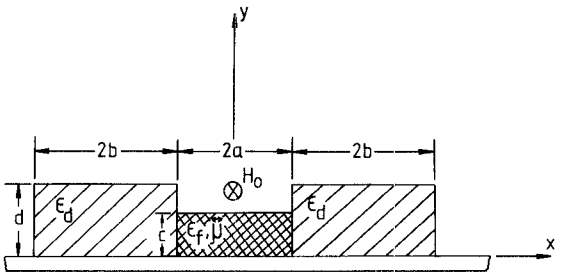

Fig. 1. Ferrite-filled coupled image line structure.

It is this structure which will be investigated theoretically in this paper. A simplified analysis of the coupled image line structure using the effective dielectric constant method is used to produce nonreciprocal propagation constants and field distributions. It will be shown that nonreciprocal coupling (i.e., circulation) can be developed over reasonable lengths of the coupled section.

II. Analysis

The effective dielectric constant method has been used previously to analyze a number of isotropic and nonreciprocal dielectric waveguide structures [6], [9]–[11] and will therefore not be described in detail here. In relation to the structure of Fig. 1, the ferrite and dielectric regions are modeled by separate slab structures, as shown in Fig. 2(a) and (b), respectively, each infinite in the x direction. The values of the effective dielectric constants obtained from each slab are used in the hypothetical structure of Fig. 2(c) to produce the propagation constants of the original structure.

A. Longitudinally Magnetized Ferrite

To obtain the effective dielectric constants of the model ferrite slab structure of Fig. 2(a), it is necessary to know the form which the nonreciprocal propagation constants will take in relation to the gyromagnetic elements of the ferrite. A simplified form is discussed as follows assuming that the material is lossless, extends to infinity in both the x and the z direction, and is bounded by either electric or magnetic walls at $y = 0$ and $y = c$.

Maxwell's equations describing propagation within the ferrite medium can be written in the following form:

$$\nabla \times \boldsymbol{E} = -j\omega[\mu]\boldsymbol{H} \qquad \nabla \times \boldsymbol{H} = j\omega\epsilon\boldsymbol{E} \tag{1}$$

Manuscript received July 14, 1986; revised February 21, 1987. This work was supported in part by the U.K. Science and Engineering Research Council.

The authors are with the Department of Electrical and Electronic Engineering, Paisley College of Technology, Paisley, PA1 2BE, Scotland.

IEEE Log Number 8714790.

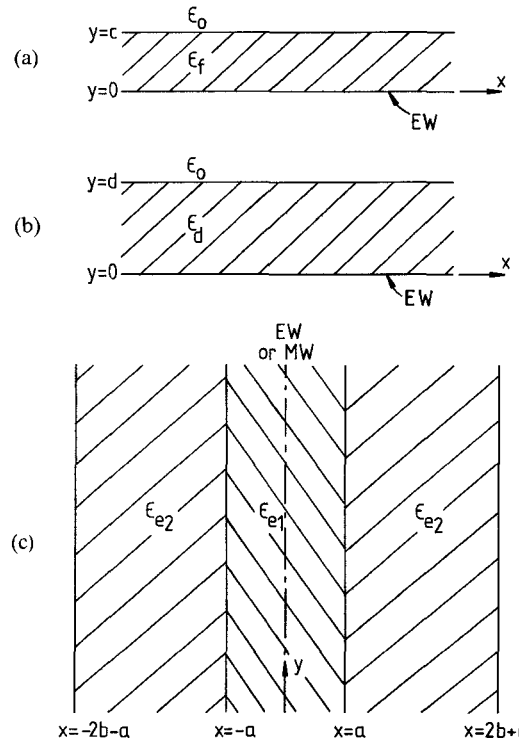

Fig. 2. Computation of the effective dielectric constants. (a) Ferrite slab structure for computing ϵ_{e1}. (b) Dielectric slab structure for computing ϵ_{e2}. (c) Hypothetical structure with electric or magnetic wall symmetry.

where

$$[\mu] = \begin{bmatrix} \mu & j\kappa & 0 \\ -j\kappa & \mu & 0 \\ 0 & 0 & \mu_0 \end{bmatrix} \tag{2}$$

and

$$\mu = \mu_0\left(1 + \frac{\omega_m\omega_0}{\omega_0^2 - \omega^2}\right) \qquad \kappa = -\frac{\mu_0\omega_m\omega}{\omega_0^2 - \omega^2} \tag{3}$$

and $\omega_0 = \gamma H_0$, $\omega_m = \gamma M_s$, $\gamma = 2.21 \times 10^5$ (rad/s)/(A/m). An expansion of (1) yields the following characteristic equation:

$$\nabla_t^4 + \nabla_t^2\left[\omega^2\mu_0\epsilon_f\left(1 + \frac{\mu_f}{\mu_0}\right) - \left(1 + \frac{\mu_0}{\mu}\right)k_z^2\right] - 2\omega^2\mu_0\epsilon_f k_z^2 + \frac{\mu_f}{\mu_0}\left(\omega^2\mu_0\epsilon_f\right)^2 + \frac{\mu_0}{\mu}k_z^4 = 0 \tag{4}$$

where we have defined $\nabla_t^2 = [\partial^2/\partial x^2 + \partial^2/\partial y^2]$ and $\mu_f = \mu - \kappa^2/\mu$, with k_z the propagation constant of the ferrite slab structure.

As expected, (4) contains the simple special cases and a useful approximation is also possible. First, if $\partial/\partial x = \partial/\partial y = 0$, (4) reduces to $k_z^2 - \omega^2\epsilon_f(\mu \pm \kappa) = 0$, as expected. Also, if $\kappa = 0$ and $\mu = \mu_0$, the medium becomes a simple dielectric and (4) reduces to $k_z^2 = \omega^2\mu_0\epsilon_f - k_f^2$, assuming $\partial/\partial x = 0$ and $\partial/\partial y = jk_f$, where k_f is the transverse propagation constant. As this is the equation for the propagation constant when the gyrotropy is reduced to zero, it is convenient at this point to denote it by the specific symbol k_z'. So we define

$$k_z'^2 = \omega^2\mu_0\epsilon_f - k_f^2. \tag{5}$$

It is well known that if an infinitely long ferrite slab is magnetized longitudinally, then the demagnetizing factor in that direction as defined by Kittel [12] is zero. Hence, saturation of the ferrite can ideally be obtained from an applied magnetic field H_0 equal to zero. This reduces the elements of the permeability tensor (3) to the following forms

$$\mu \approx \mu_0 \qquad \kappa \approx \mu_0\omega_m/\omega.$$

Hence, after some manipulation, (4) reduces to the following characteristic equation [13]:

$$\left(\omega^2\mu_0\epsilon_f - k_f^2 - k_z^2\right)^2 - \frac{\omega^2\epsilon_f\kappa^2}{\mu_0}\left(\omega^2\mu_0\epsilon_f - k_f^2\right) = 0. \tag{6}$$

Using (5), (6) can be written in the form

$$\left(k_z^2 - k_z'^2\right)^2 = \frac{\omega^2\kappa^2\epsilon_f k_z'^2}{\mu_0} \tag{7}$$

and if the propagation constant in the unbounded dielectric medium is defined by $k^2 = \omega^2\mu_0\epsilon_f$, (7) can be rewritten in the form

$$k_z^{\pm} = k_z'\left[1 \pm \frac{k\kappa}{\mu_0 k_z'}\right]^{1/2}. \tag{8}$$

It is clear that (8) simply expresses the nonreciprocal propagation constant k_z in terms of a perturbation of the isotropic propagation constant k_z' caused by the off-diagonal element of the permeability tensor.

B. Field Components

In the following analysis, which was originally developed by Marcatili [14], only the E_{mn}^y modes will be considered. Therefore, the field components present in both the ferrite and the air regions of Fig. 2(a) can be obtained from the main electric field expression, written as

$$E_y = \begin{cases} A\cos(k_f y), & 0 \leqslant y \leqslant c \\ B\exp\left[-k_a(y-c)\right], & y \geqslant c \end{cases} \tag{9}$$

assuming the plane $y = 0$ is an electric wall. Similar expressions also describe the field components in the dielectric and air regions of Fig. 2(b) but with k_f replaced by k_d, c by d, and k_a by k_a^-. Boundary conditions are hence applied to both structures (a) and (b) in Fig. 2, with the resulting transcendental equations solved to produce the effective dielectric constants ϵ_{e1} and ϵ_{e2} of the ferrite and dielectric slab structures, respectively. It should be noted that ϵ_{e1} has two solutions, corresponding to the nonreciprocity of the longitudinally magnetized ferrite as indicated by (8).

The field components describing the odd- and even-mode characteristics of the hypothetical structure of Fig. 2(c) can be written as follows, noting the presence of electric or

magnetic wall symmetry at $x = 0$:

$$E_y = \begin{cases} A\begin{Bmatrix}\sinh(k_1 x)\\ \cosh(k_1 x)\end{Bmatrix} & \begin{matrix}\text{odd}\\ \text{even}\end{matrix} \qquad 0 \leqslant x \leqslant a \\ B\cos[k_2(x-a)] + C\sin[k_2(x-2b-a)] & a \leqslant x \leqslant 2b+a \\ D\exp[-k_3(x-2b-a)] & x \geqslant 2b+a. \end{cases} \tag{10}$$

The transverse propagation constant k_2 and attenuation coefficients k_1 and k_3 in the x direction are related as follows:

$$\beta^2 = \omega^2\epsilon_{e1}\mu_0 + k_1^2 = \omega^2\epsilon_{e2}\mu_0 - k_2^2 = \omega^2\epsilon_0\mu_0 + k_3^2.$$

By applying boundary conditions at each interface of the hypothetical structure, the following eigenvalue equation is obtained:

$$[k_2\sin(k_2 2b) - k_3\cos(k_2 2b)] - k_1[\cos(k_2 2b) + (k_3/k_2)\sin(k_2 2b)] \cdot \begin{Bmatrix}\coth(k_1 x)\\ \tanh(k_1 x)\end{Bmatrix} = 0 \quad \begin{matrix}\text{odd}\\ \text{even}\end{matrix}. \tag{11}$$

The solutions of (11) are the odd- and even-mode propagation constants of the original coupled image line structure.

The above analysis reduces to that presented in [11] for directly connected coupled image lines when the ferrite becomes dielectric (i.e., $\kappa = 0$) and to coupled image guide when c/d equals zero [9].

III. Nonreciprocal Coupling

We adopt the notation $\beta_e^{\pm}$ and $\beta_o^{\pm}$ for the propagation constants of the even and odd modes, respectively. The positive and negative superscripts indicate the orientation of propagation (forward or reverse) with respect to the direction of the applied magnetic field H_0. The relative differences between the values of the even- and odd-mode propagation constants describing the forward wave, β_e^+ and β_o^+, respectively, and those relating to the negative wave, β_e^- and β_o^-, are the criteria for obtaining the necessary conditions for nonreciprocal coupling ($S_{21}^{\pm}$). The following conditions, therefore, must be fulfilled [6]:

$$(\beta_e^+ - \beta_o^+)L = 2n\pi, \qquad n = 0,1,2,3,\cdots \tag{12}$$

$$(\beta_e^- - \beta_o^-)L = (2m+1)\pi, \qquad m = 0,1,2,3,\cdots \tag{13}$$

where L is the length of the nonreciprocal coupling section. The nonreciprocal coupling parameters can hence be calculated using the following expression:

$$|S_{21}^{\pm}| = |\sin(\beta_e^{\pm} - \beta_o^{\pm})L/2|. \tag{14}$$

The following section describes some results of nonreciprocal coupling present in the coupled image line structure separated by longitudinally magnetized ferrite.

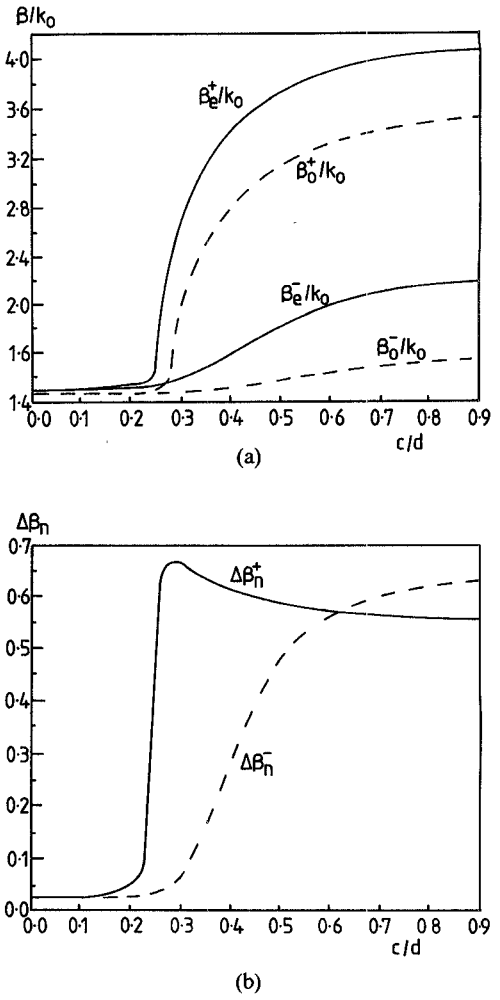

Fig. 3. Normalized nonreciprocal (a) propagation constants and (b) differential propagation constants versus c/d. $\epsilon_f = 13.0$, $M_s = 4000$ A/cm, $\kappa/\mu_0 = 0.5$, $\epsilon_d = 2.56$, $2a = 3.0$ mm, $2b = 4.8$ mm, $d = 2.4$ mm, and frequency = 33.5 GHz.

IV. Results

In the analysis, coupled image lines consisting of low-dielectric-constant material (cross-linked polystyrene with $\epsilon_d = 2.56$) and high-dielectric-constant material (alumina with $\epsilon_d = 9.8$) were considered. In both cases, the ferrite employed in the coupling structures had the same material characteristics, i.e., $M_s = 4000$ A/cm, $\epsilon_f = 13.0$, and the magnitude of κ/μ_0 assumed to be equal to 0.5.

A. $\epsilon_d = 2.56$

Fig. 3(a) shows curves of the normalized nonreciprocal propagation constants of the even and odd modes of the ferrite-loaded structure as a function of normalized ferrite height c/d assuming an image line with $\epsilon_d = 2.56$ and having cross-sectional dimensions of 4.8 mm × 2.4 mm, a ferrite of width equal to 3.0 mm, and assuming an operating frequency of 33.5 GHz. It is interesting to note from Fig. 3(a) that no appreciable nonreciprocity in the propagation constants is indicated for ferrite heights corresponding to 0.5 mm or less. This is clearly shown in Fig. 3(b), where the normalized differential propagation constants

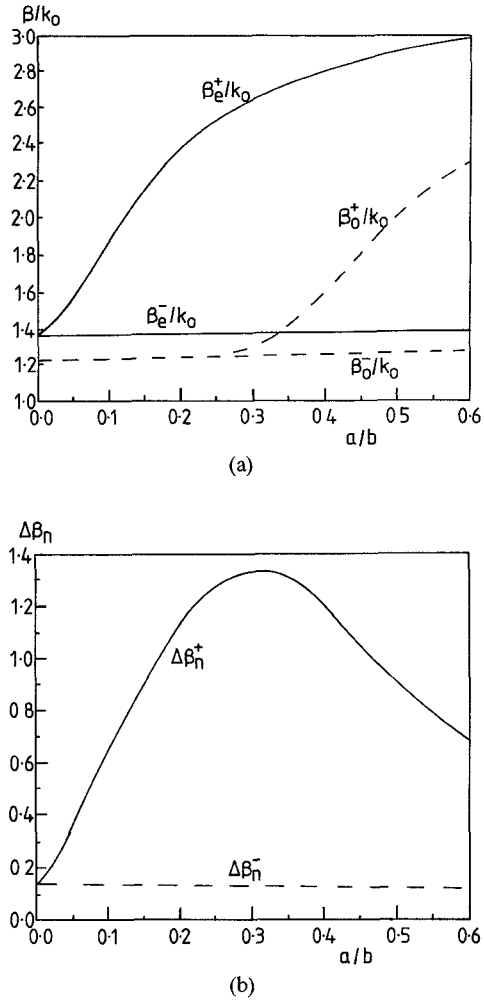

Fig. 4. Normalized nonreciprocal (a) propagation constants and (b) differential propagation constants versus a/b. $\epsilon_d = 2.56$, $2b = 4.8$ mm, $c = 0.8$ mm, $d = 2.4$ mm, and frequency = 33.5 GHz.

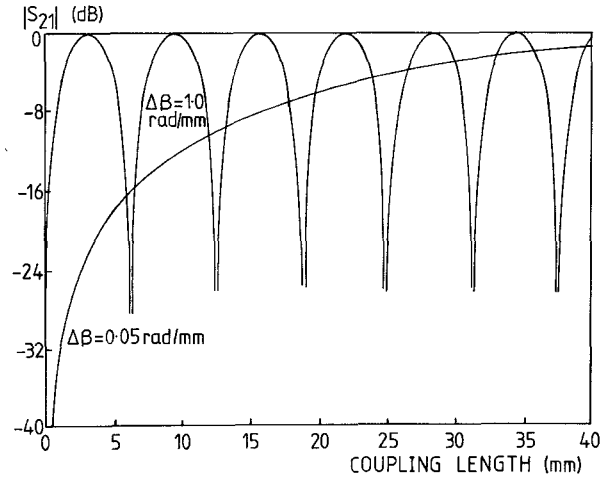

Fig. 5. Coupling parameters versus coupling length for $\Delta\beta = 0.05$ and 1.0 rad/mm.

$\Delta\beta_n^{\pm} \equiv (\beta_e^{\pm} - \beta_o^{\pm})/k_o$ are also plotted as a function of normalized ferrite height. Here, it can be seen that between ferrite heights of 0.5 mm and 0.7 mm there is a large increase in the value of $\Delta\beta_n^+$, which then decreases and eventually equals the value of $\Delta\beta_n^-$, for when the ferrite is 1.5 mm in height. It should also be noted that as the ferrite height approaches that of the dielectric image line ($c/d \rightarrow 1$), there is no appreciable change in the values of the odd- and even-mode propagation constants.

The normalized nonreciprocal propagation constants are also plotted as a function of normalized ferrite width a/b, as shown in Fig. 4(a) for a fixed ferrite height of 0.8 mm. The corresponding curves of differential propagation constant are plotted in Fig. 4(b). Again, it is interesting to note that the $\Delta\beta_n^+$ curve reaches a maximum value, corresponding to when the ferrite width is equal to 1.5 mm.

In choosing ferrite dimensions which will produce conditions of nonreciprocal coupling achievable over a reasonable length of coupling, the relative values of $\Delta\beta_n^+$ to $\Delta\beta_n^-$ are important. For instance, in Fig. 5 the coupling parameters in dB are shown as a function of coupling length for two different values of $\Delta\beta$. It can be seen that if $\Delta\beta$ is small, then a long length of coupling is required in which to obtain complete coupling. Alternatively, too large a value of $\Delta\beta$, although necessitating only a small length for complete coupling, would result in a narrow bandwidth being produced. It was found that for a ferrite having cross-sectional dimensions of 3.0 mm × 0.8 mm, nonreciprocal coupling would occur for a chosen coupling length of 41.4 mm, which satisfies both conditions stated in (12) and (13).

The nonreciprocal dispersion characteristics for this structure are shown in Fig. 6(a) for the frequency range 26.5–40 GHz, with the corresponding differential propagation constants plotted in Fig. 6(b). Marked on Fig. 6(b) as broken lines are multiple values of $\Delta\beta$ required to give alternate conditions of complete coupling ($S_{21} = 1$) and zero coupling ($S_{21} = 0$) for a coupling length of 41.4 mm. The ideal characteristics would be, for example, for $\Delta\beta^+$ to have a value corresponding to $S_{21} \approx 0$ over the complete frequency range while $\Delta\beta^-$ has a value corresponding to $S_{21} \approx 1$, or vice versa. This is equivalent to satisfying (12) and (13) over the calculated frequency range. A plot of the resulting nonreciprocal coupling parameters is shown in Fig. 7 calculated using (14).

The distributions of E_y within the ferrite and dielectric regions are shown in Fig. 8(a) and (b) at the points $z = 0.0$ mm and $z = 41.4$ mm, respectively. In these figures, the magnitude of E_y is plotted as a function of the x coordinate. It is clear from these diagrams that the low dielectric constant of the image line results in the effective dielectric constant of the ferrite region being larger than that of the dielectric region. This is indicated in both (a) and (b) of Fig. 8, with the field concentrated in one half of the ferrite region (corresponding to transmission at points $z = 0.0$ mm and $z = 41.4$ mm). It was found that for heights of ferrite larger than 0.5 mm, the effective dielectric constant of the ferrite slab structure is greater than that of the dielectric structure. It is then necessary to replace the hyperbolic functions of (10) which refer to propagation in the ferrite with trigonometric functions, and vice versa for the functions describing the fields in the dielectric.

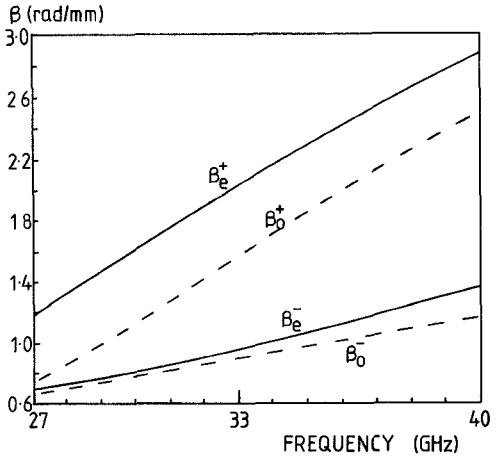

(a)

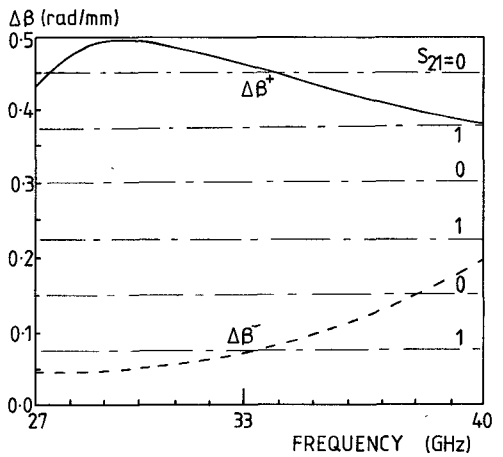

(b)

Fig. 6. Nonreciprocal (a) dispersion and (b) differential dispersion characteristics. $\epsilon_d = 2.56$, $2a = 1.0$ mm, $2b = 4.8$ mm, $c = 0.8$ mm, and $d = 2.4$ mm.

The larger field concentration within the ferrite region for forward propagation compared to that for reverse propagation is due to the larger value of the effective dielectric constant. It should also be noted that for reverse propagation, the field couples from one side to the other over the selected coupling length 41.4 mm.

B. $\epsilon_d = 9.8$

An image line consisting of a higher dielectric constant material (alumina with $\epsilon_d = 9.8$) and having cross-sectional dimensions of 2.0 mm × 1.0 mm was also considered in the analysis. The nonreciprocal dispersion characteristics of this structure are plotted in Fig. 9(a) for a ferrite having cross-sectional dimensions of 1.5 mm × 0.6 mm. The corresponding curves of differential propagation constants are shown in Fig. 9(b) and indicate a much smaller relative difference in value between $\Delta\beta^+$ and $\Delta\beta^-$ compared to those for the similar structure with lower dielectric constant image lines.

To obtain nonreciprocal coupling at the center frequency of 33.5 GHz, a minimum coupling length of 45.8 mm was found to be necessary. Lines showing the values of $\Delta\beta$ necessary to produce alternate conditions of complete and zero coupling corresponding to the coupling length of 45.8 mm are indicated on Fig. 9(b). The nonreciprocal coupling parameters are shown in Fig. 10 calculated using (14). It is interesting to note in Fig. 10 that the curve of S_{21}^+ indicates a large bandwidth at approximately − 15 dB. The reasons

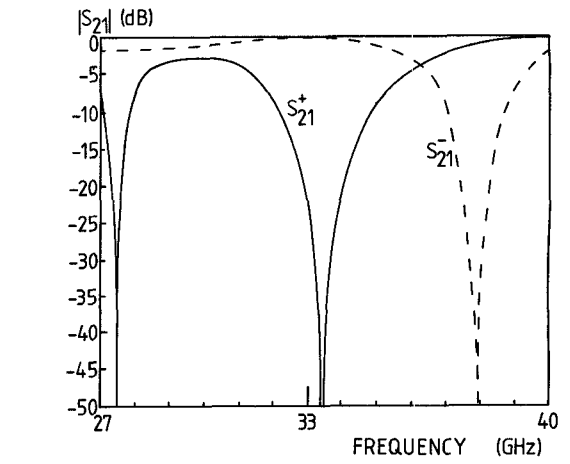

Fig. 7. Nonreciprocal coupling parameters for coupling length equal to 41.4 mm. $\epsilon_d = 2.56$, $2a = 1.0$ mm, $2b = 4.8$ mm, $c = 0.8$ mm, and $d = 2.4$ mm.

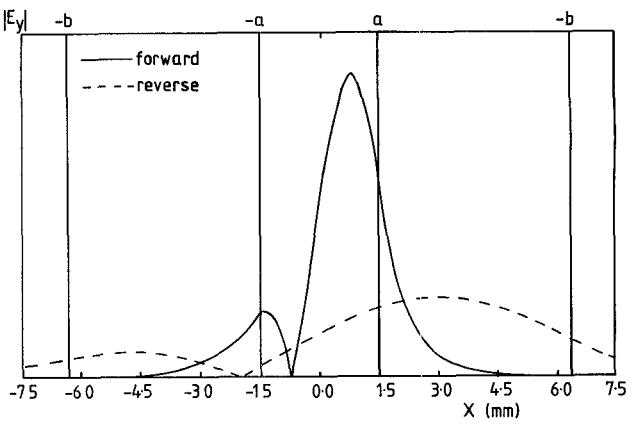

(a)

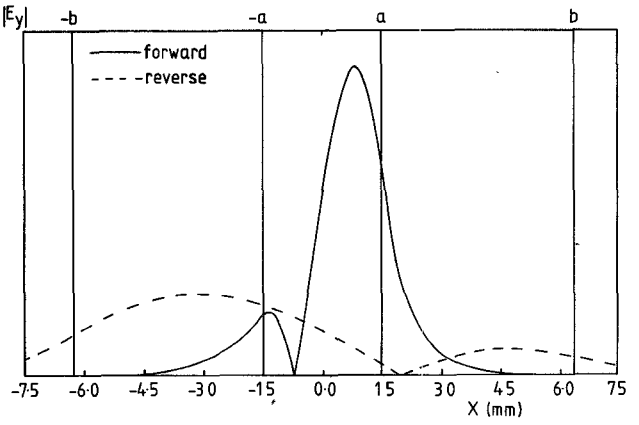

(b)

Fig. 8. Field distribution for forward and reverse propagation at (a) $z = 0.0$ mm and (b) $z = 41.4$ mm. $\epsilon_d = 2.56$, $2a = 1.0$ mm, $2b = 4.8$ mm, $c = 0.8$ mm, $d = 2.4$ mm, and frequency = 33.5 GHz.

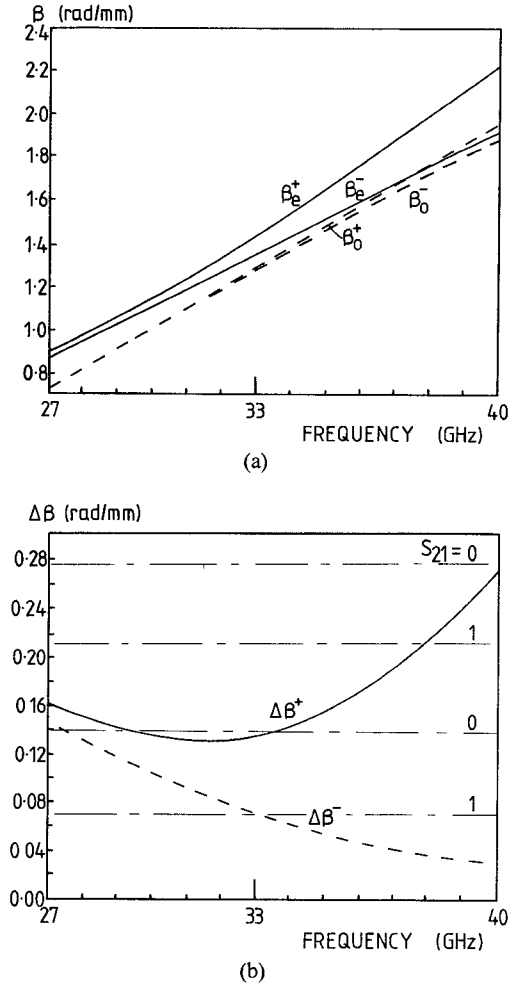

Fig. 9. Nonreciprocal (a) dispersion and (b) differential dispersion characteristics. $\epsilon_f = 13.0$, $M_s = 4000$ A/cm, $\kappa/\mu_0 = 0.5$, $\epsilon_d = 9.8$, $2a = 1.5$ mm, $2b = 2.0$ mm, $c = 0.6$ mm, and $d = 1.0$ mm.

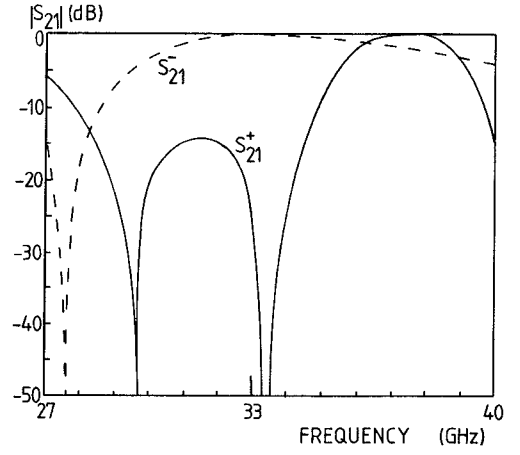

Fig. 10. Nonreciprocal coupling parameters for coupling length equal to 45.8 mm. $\epsilon_d = 9.8$, $2a = 1.5$ mm, $2b = 2.0$ mm, $c = 0.6$ mm, and $d = 1.0$ mm.

for this are that the curve corresponding to $\Delta\beta^+$ in Fig. 9(b) intersects the same zero coupling line at both 29.7 GHz and 33.5 GHz and does not markedly deviate from the "zero line" between these frequency values.

The distributions of E_y plotted along the x coordinate at both, $z = 0.0$ mm and $z = 45.8$ mm are shown in Fig.

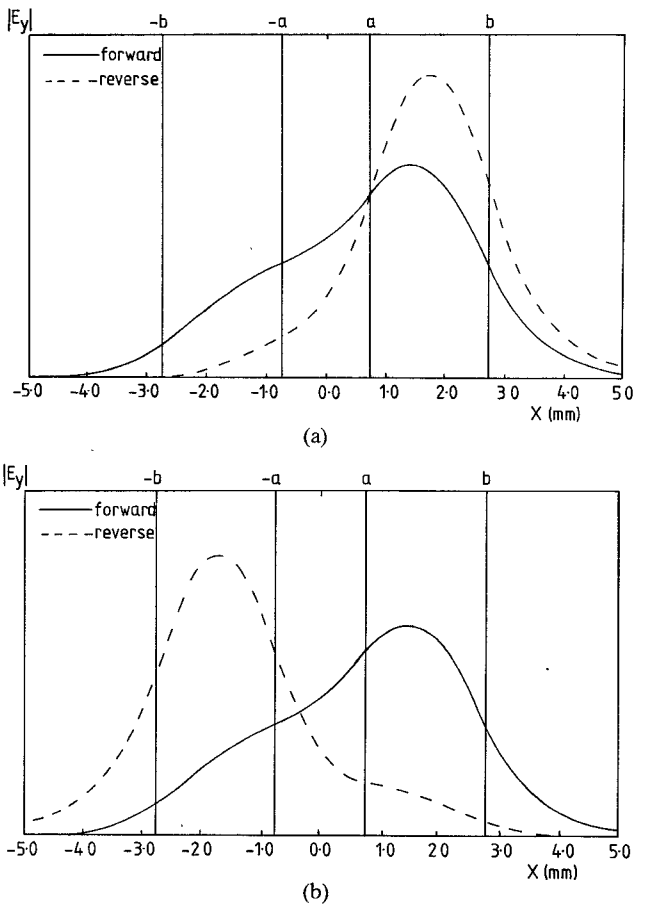

Fig. 11. Field distribution for forward and reverse propagation at (a) $z = 0.0$ mm and (b) $z = 45.8$ mm. $\epsilon_d = 9.8$, $2a = 1.5$ mm, $2b = 2.0$ mm, $c = 0.6$ mm, $d = 1.0$ mm, and frequency = 33.5 GHz.

11(a) and (b), respectively. It is clear from both these diagrams that for reverse propagation the wave shifts from the transmission arm of the coupled line structure to the coupled arm over the length of coupling and that for forward propagation the wave remains unaffected, guided by the transmission arm. Because the effective dielectric constant of the dielectric region is larger than that of the ferrite region, the field is therefore concentrated in the image lines.

Colleagues have recently presented experimental results of nonreciprocal coupling in this type of image line structure [8]. The experimental structure consisted of two low-dielectric-constant image lines ($\epsilon_r = 2.56$) with a straight coupling section of length 40 mm and a separation equal to 3 mm. A ferrite slab of dimensions 28 mm × 3 mm × 1mm was placed between the image lines and magnetized longitudinally by an applied magnetic field strength approximately equal to 159 A/cm. The results showed that power switched from one output port to the other by reversing the applied magnetic field, with a minimum differential insertion loss of 15 dB developed over a bandwidth of 1.5 GHz between 30 GHz and 35 GHz.

Direct comparison between the results produced from the experimental and theoretical structures is not possible because of experimental factors such as curved sections, reciprocal coupling sections, and material losses, which

were not taken into consideration in the analytical model. However, the results of the analysis demonstrate that a longitudinally magnetized ferrite can cause nonreciprocal coupling between the image lines over a realistic length of coupling.

V. Conclusions

An analysis based on the effective dielectric constant method has been used to study the nonreciprocal coupling properties of a coupled image line structure separated by a longitudinally magnetized ferrite slab. Examples of nonreciprocal dispersion characteristics have been presented and coupling lengths necessary for conditions of nonreciprocal coupling predicted. Nonreciprocity has been substantiated by plots of the field distributions within the structure, which show a power transfer from one line to the other. Confirming previous initial experimental results, these structures are characterized by incorporating "weakly" magnetized ferrites and realistic lengths of coupling to produce 4-port circulation. These concepts have applications in other structures and at higher frequencies.

References

[1] R. A. Stern and R. W. Babbitt, "Dielectric millimeter-wave ferrite devices," *IEEE Trans. Magn.*, vol. MAG-18, no. 6, pp. 1592–1594, Nov. 1982.

[2] R. Glockler, "Millimetre-wave dielectric waveguide ferrite phase shifter with longitudinal magnetisation," *Electron. Lett.*, Sept. 12, 1985, vol. 21, no. 9, pp. 827–829.

[3] B. Lax and K. J. Button, *Microwave Ferrites and Ferrimagnetics*. New York: McGraw-Hill, 1962.

[4] S. W. Yun and T. Itoh, "A distributed millimetre-wave isolator using non-reciprocal coupling structure," *Int. J. Infrared and Millimeter Waves*, vol. 5, no. 6, pp. 775–792, 1984.

[5] I. Awai and T. Itoh, "Coupled-mode theory analysis of distributed nonreciprocal structures," *IEEE Trans. Microwave Theory Tech.*, vol. MTT-29, pp. 1077–1087, Oct. 1981.

[6] S. W. Yun and T. Itoh, "Non-reciprocal wave propagation in a hollow image guide with a ferrite layer," *Proc. Inst. Elec. Eng.*, vol. 132, pt. H, no. 4, pp. 222–226, July 1985.

[7] L. E. Davis and D. B. Sillars, "Millimetric nonreciprocal coupled-slot finline components," *IEEE Trans. Microwave Theory Tech.*, vol. MTT-34, July 1986.

[8] A. Nicol and L. E. Davis, "Non-reciprocal coupling in dielectric image lines," *Proc. Inst. Elec. Eng.*, vol. 132, pt. H, no. 4, pp. 269–270, July 1985.

[9] W. V. McLevige, T. Itoh, and R. Mittra, "New waveguide structures for millimeter-wave and optical integrated circuits," *IEEE Trans. Microwave Theory Tech.*, vol. MTT-23, pp. 788–794, Oct. 1975.

[10] J. F. Miao and T. Itoh, "Hollow image guide and overlayed image guide coupler," *IEEE Trans. Microwave Theory Tech.*, vol. MTT-30, pp. 1826–1831, Nov. 1982.

[11] D. I. Kim *et al.*, "Directly connected image guide 3-dB couplers with very flat couplings," *IEEE Trans. Microwave Theory Tech.*, vol. MTT-32, pp. 621–627, June 1984.

[12] C. Kittel, "On the theory of ferromagnetic resonance absorption," *Phys. Rev.*, vol. 73, pp. 155–161, 1948.

[13] D. B. Sillars, "Non-reciprocal coupled-slot devices in fin-line structures for millimetric wavelengths," CNAA Ph.D. thesis, Paisley College of Technology, Scotland, 1985.

[14] E. A. J. Marcatili, "Dielectric rectangular waveguide and directional coupler for integrated optics," *Bell Syst. Tech. J.*, vol. 48, pp. 2071–2102, 1969.

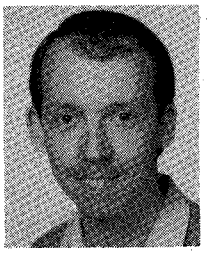

David B. Sillars (M'83) was born in Irvine, Ayrshire, Scotland, on August 22, 1960. He received the B.Sc. degree (with honors) and the Ph.D. degree, both in electrical and electronic engineering, from Paisley College of Technology, Scotland, in 1982 and 1986, respectively.

At present, he is employed as an SERC Research Assistant in the Department of Electrical and Electronic Engineering, Paisley College of Technology. His current research interests are in millimeter-wave nonreciprocal components involving finline and image-line technology.

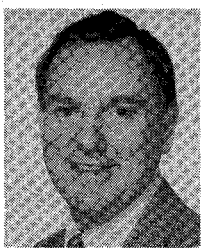

Lionel E. Davis (SM'65) received the B.Sc. and Ph.D. degrees from the University of Nottingham and the University of London in 1956 and 1960, respectively.

From 1959 to 1964, he was with Mullard Research Laboratories, Redhill, England, and from 1964 to 1972, he was an Assistant Professor and then Associate Professor of Electrical Engineering at Rice University, Houston, TX. In 1972, he joined Paisley College, Scotland, as Head of the Department of Electrical and Electronic Engineering, where he is now also Dean of Engineering. His current research interests are in millimetric-wave components and liquid crystal electro-optical switching for optical image processing.

Dr. Davis has served on the Council and other committees of the Institution of Electrical Engineers and on several committees of the Science and Engineering Research Council. He has been a Visiting Professor at University College London (1970/71) and the University of California at San Diego (1978/79) and a Consultant for Bendix Research Laboratories (1966–68). He was a founding member of the Houston Chapter of the Microwave Theory and Techniques Society.